



## **SILAR Sensitization as an Effective Method for Making Efficient Quantum Dot Sensitized Solar Cells**

Mahmoud Samadpour<sup>a\*</sup>, Mehdi Molaei<sup>b</sup>

<sup>a</sup>*Department of Physics, K.N.Toosi University of Technology, Tehran, Iran*

<sup>b</sup>*Department of Physics, Vali-e-Asr University, Rafsanjan, Iran*

### **Article History**

Received: 24 Oct. 2013 Received in revised form: 11 April 2014 Accepted: 29 April 2014 Available online: 17 Sep. 2014

### **A B S T R A C T**

CdSe quantum dots were in situ deposited on various structures of TiO<sub>2</sub> photoanode by successive ionic layer adsorption and reaction (SILAR). Various sensitized TiO<sub>2</sub> structures were integrated as a photoanode in order to make quantum dot sensitized solar cells. High power conversion efficiency was obtained; 2.89 % ( $V_{oc}=524$  mV,  $J_{sc}=9.78$  mA/cm<sup>2</sup>, FF=0.56) for the cells sensitized by SILAR method. Also, all the cells showed rather high efficiencies (over 2.65%) regardless of their structure. Here the simple SILAR deposition was performed at room temperature, which introduces it as a cost effective method for large scale production. Regarding the considerable efficiencies obtained for various structures, pointed out that SILAR deposition can be introduced as an effective method for making efficient quantum dot sensitized solar cells.

**Keywords:** Solar cell, SILAR, CdSe, Quantum dot

### **1. Introduction**

In the Dye sensitized solar cells (DSCs), molecular dyes are used as light absorbing materials to produce photogenerated electrons. Photogenerated electrons are injected into a wide band gap semiconductor like TiO<sub>2</sub> which transfer the electrons to the external circuit. Dye molecules are regenerated by a redox electrolyte which acts as a hole transporting media [1]. Recently, the unique properties of semiconductor quantum dots in comparison to convenient dyes like ease of synthesization, tunable band gap by controlling their size, high molar extinction coefficients and multiple exciton generation in colloidal QDs [2,3] has increased the interest toward QDs as sensitizers in quantum dot

sensitized solar cells (QDSCs) [4-9]. In spite of the mentioned advantages of QDs, the efficiency of QDSCs is currently lower than the efficiencies of conventional DSCs [10,11] and some parameters like charge injection and recombination, redox electrolyte composition, counter electrode (CE) catalytic properties and uniform deposition of QDs onto the TiO<sub>2</sub> surface have not been optimized yet [11-13]. The literature points out that one of the key differences between Dye and QD sensitized solar cells is the sensitization procedure. In DSCs, dye molecules are effectively adsorbed on the photoanode by soaking the TiO<sub>2</sub> film in the dye solution, while in the QDSCs, the uniform deposition of QDs on TiO<sub>2</sub> surface is

\* Corresponding author. Email: [samadpour@kntu.ac.ir](mailto:samadpour@kntu.ac.ir)

still a challenge. So far, various methods containing direct or linker molecule mediated adsorption of pre synthesized colloidal QDs on  $\text{TiO}_2$  have been utilized in order to deposit QDs on the  $\text{TiO}_2$  photoanode in QDSCs. Also, direct growth of QDs on the  $\text{TiO}_2$  surface by SILAR or chemical bath deposition (CBD) methods have recently used for sensitizing electrodes by semiconductor QDs [12-19]. Reviewing the literature shows that less than 20 % of  $\text{TiO}_2$  surface is covered by QDs in the case of direct adsorption method, and consequently, low efficiency cells are obtained by this method [12]. In the case of linker mediated adsorption, one head of the linker molecule is attached to the surface of  $\text{TiO}_2$ , while the other head is attached to QDs, and consequently, more deposition of QDs is obtained in comparison with direct adsorption. In the case of linker mediated adsorption, in spite of higher deposition of QDs, there is still a considerable surface of  $\text{TiO}_2$  photoanode which is not covered by QDs. Here, linker molecules act as an intermediate layer between QDs and  $\text{TiO}_2$  which disturb the direct electron transfer from photoexcited QDs through the  $\text{TiO}_2$  photoanode. In both cases of SILAR and CBD methods, there is a high loading of QDs on  $\text{TiO}_2$  surface and high photocurrents is usually obtained for the solar cells. In the CBD method all the QD precursors should diffuse into the pores of the mesoporous  $\text{TiO}_2$  structure simultaneously in order to make a homogeneous deposition of QDs on the photoanode. This is particularly a challenge in the case of structures with very small pores. Also, CBD is usually performed in low temperature condition for controlling the QDs growth rate more precisely. Performing CBD in low temperature conditions, limits the large scale and cost effective production of the cells. Here, we use SILAR method at room temperature for sensitizing various structures of photoanode by CdSe QDs. We show by applying SILAR deposition method that not only high QD loading on  $\text{TiO}_2$  anode is obtained, but also mesoporous structure of  $\text{TiO}_2$  with small pores can be sensitized effectively. Here, high efficiency cells are obtained by SILAR method. Also room temperature deposition introduces this method as a potential

candidate for large scale production of the QDSCs.

## 2. Experimental section

### 2.1. Electrode preparation

Three different  $\text{TiO}_2$  pastes were used to make photo electrodes. The first one was “18NR-T Dyesol paste” which contains 20 nm  $\text{TiO}_2$  nanoparticles and leads to high surface area mesoporous structures with small pores; we name this paste as “P20”. The second paste was “18NR-AO Dyesol paste” which contains 20-450 nm  $\text{TiO}_2$  nanoparticles; we name this paste as “P20-450”. The third one was made by  $\text{TiO}_2$  nanorods as follows:

For synthesizing  $\text{TiO}_2$  nanorods, Titanium foils were cleaned by sonication in acetone and deionized (DI) water for 10 minutes and then dried in nitrogen stream. Ti foils were then immersed in 10 mL of 30% W hydrogen peroxide solution and kept at 80°C for 72 h. Samples were then removed and rinsed with DI water and dried in air. Heat treatment process was performed at 450°C and kept at this temperature for 1 h. These nanorods were scratched from the Ti substrate and used to make nanorod based pastes. For the third paste, 1gr of ethyl cellulose was dissolved in 12.5 ml ethanol assisted by ultrasonication. The paste was prepared by milling 0.2 gr  $\text{TiO}_2$  nanorods and 1 ml of ethyl cellulose in ethanol in a mortar for 30 minutes while 1ml of terpineol was added drop by drop during the milling process. We name this paste as “NR”. Three different electrode configurations were prepared as photoanode in QDSCs by using these three kinds of  $\text{TiO}_2$  Pastes. Photoanodes were deposited by doctor-blade method on transparent conducting fluorine doped tin oxide (FTO) glass substrates (sheet resistance  $\sim 15 \Omega/\text{cm}^2$ ) and sintered at 450 °C, for 1 hour.

### 1.2. Electrode Sensitization

The SILAR process was carried out following the method developed by [17]. In short, a 0.03 M  $\text{Cd}(\text{NO}_3)_2$  in ethanol was used as the  $\text{Cd}^{+2}$  precursor. A 0.03 M selenide solution was prepared by dissolving of 0.2 gr  $\text{SeO}_2$  and 0.27 gr  $\text{NaBH}_4$  in 60 ml ethanol under  $\text{N}_2$  atmosphere and used as a  $\text{Se}^{2-}$  precursor. For sensitization,

electrodes were dipped successively in these solutions under  $N_2$  atmosphere. One SILAR cycle for CdSe deposition consisted of 30 second dipping the  $TiO_2$  working electrode into the  $Cd^{2+}$  precursor and subsequently into the selenide solution, during 30 second. Following each bath, the photoanode was rinsed by immersion in the pure ethanol to remove the chemical residuals from the surface and then dried with a  $N_2$  gun.

In order to improve the stability and performance of cells, all the samples were deposited with ZnS protective coating [18], after SILAR, by twice dipping alternately into 0.1M  $Zn(CH_3COO)_2$  and 0.1M  $Na_2S$  solutions for 1 min/dip and drying by nitrogen flow.

### 2.3. Preparation of QDSC

The cells were prepared by sandwiching the  $Cu_2S$  counter electrode and a QD-sensitized electrode using a scotch spacer (thickness 50  $\mu m$ ) and permeating with polysulfide electrolyte. Polysulfide electrolyte was 1 M  $Na_2S$ , 1 M S, and 0.1 M NaOH solution in Milli-Q ultrapure water.

We used  $Cu_2S$  counter electrodes, clamping the sensitized electrode and the counter electrode. The  $Cu_2S$  counter electrodes were prepared by immersing brass in HCl solution at 70°C for 5 min and subsequently dipping it into polysulfide solution for 3 min, resulting in a porous  $Cu_2S$  electrode.

### 2.4. Photoanode and Solar Cell Characterization

J-V curves and Applied Bias Voltage Decay (ABVD) measurements [20] were carried out with a FRA equipped PGSTAT-30 from Autolab. J-V measurements were carried out using mask (a little smaller than photoanode) and no antireflective layer was used. Cells were illuminated using a solar simulator at AM1.5 G, where the light intensity was adjusted to one sun intensity (100  $mW/cm^2$ ).

Incident photon to electron conversion efficiency (IPCE) measurements have been performed employing a 150 W Xe lamp coupled with a monochromator while the photocurrent was measured using an optical power meter 70310 from Oriel Instruments.

### 3. Results and discussion

SEM micrograph of  $TiO_2$  nanoparticles: (P20 (20 nm), P20-450 (20-450) nm) and nanorods (NR) is shown in Figure 1. All samples have nano structure and consequently enough surface area for QDs loading is expected in all samples.

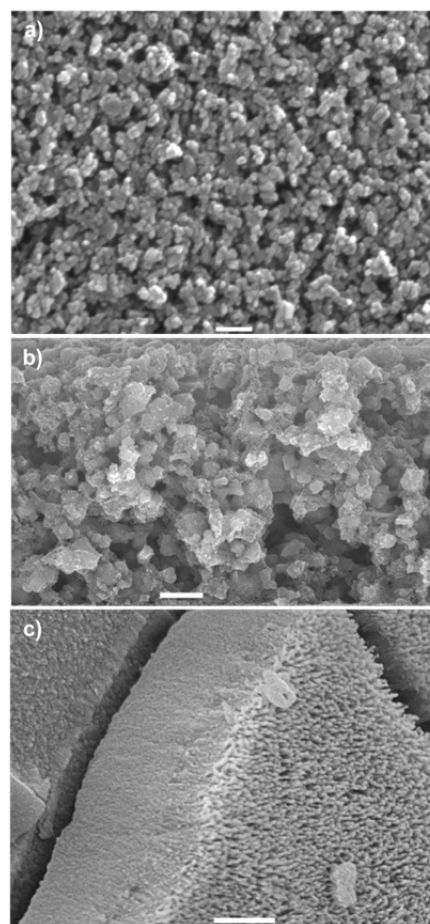


**Fig. 1.** SEM micrograph of  $TiO_2$  nanoparticles with the size of 20 nm (P20) (a), 20-450 nm (P20-450) (b) and cross section of  $TiO_2$  nanorods (NR), Scale bar is 100 nm, 1 micron and 2 microns in figure a, b and c respectively.

Crystalline structure of  $TiO_2$  nanorods was investigated by X-ray diffraction (XRD) spectrum of samples. From Figure 2, it can be seen clear peaks which are characteristic of the  $TiO_2$  anatase phase.

Morphology of the  $Cu_2S$  CE is presented in Figure 3. As it can be seen, CE has a porous structure which leads to enough catalytic sites to reduce the oxidized polysulfide electrolyte.

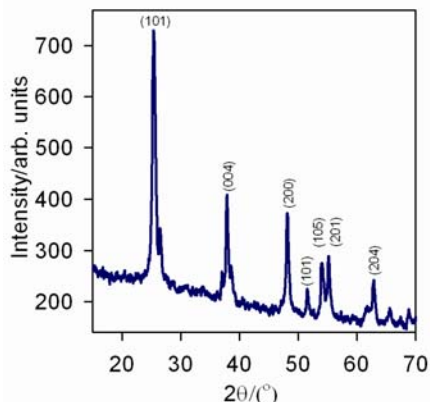


**Fig. 2.** XRD spectrum of TiO<sub>2</sub> nanorods, crystalline planes are related to anatase crystalline structure of the TiO<sub>2</sub>.

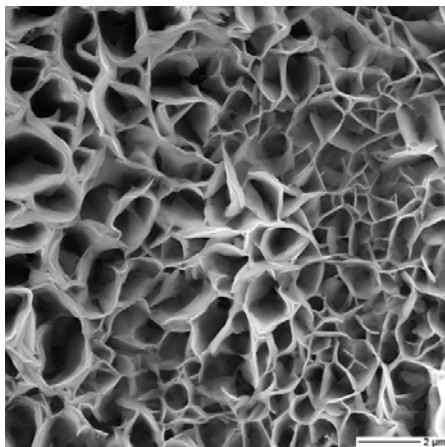


**Fig. 3.** SEM micrograph of the Cu<sub>2</sub>S counter electrodes with porous structures. Scale bar is 2 microns.

Three different TiO<sub>2</sub> pastes: P20, P20-450 and NR, see experimental section for the details, are used to make various structure of electrodes. Using Dr-Blade method 2 layers of TiO<sub>2</sub> paste was deposited on FTO substrate. These different structures were sensitized by 7 SILAR cycles of CdSe quantum dots and then coated with ZnS; see the experimental section. Figure 4 shows the current-voltage characteristic of the cells with various structures tested under standard conditions (100 mW/cm<sup>2</sup> AM 1.5G).

Table 1 shows the solar cell parameters obtained for these QDSCs: photocurrent  $j_{sc}$ , open circuit

voltage  $V_{oc}$ , fill factor  $FF$ , and efficiency  $\eta$ , as a function of the different photoanode structures.

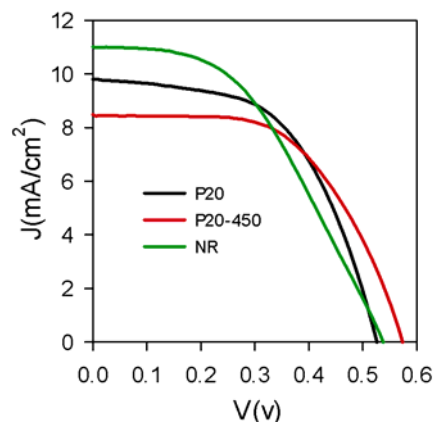


**Fig. 4.** J-V curves for SILAR sensitized cells with P20, P20-450 and NR structures.

**Table 1.** Photovoltaic parameters of the QDSCs as a function of the different cell structures tested under standard conditions (100 mW/cm<sup>2</sup> AM(air mass) 1.5G(global)).

Cell	$V_{oc}$ (mV)	$J_{sc}$ (mA/cm <sup>2</sup> )	FF	E (%)
P20	524	9.78	0.56	2.89
P20-450	575	8.48	0.56	2.74
NR	539	11.1	0.44	2.65

Using various structures, the high efficiencies were obtained in P20 (2.89%), P20-450 (2.74%) and NR (2.65%) structures.

As can be seen from Table 1, all samples have open circuit voltages of more than 500 mV, and NR samples have more current densities in comparison with P20 and P20-450 structures. The surface area of the cells was measured by the BET method and is indicated in Table 2.

**Table 2.** BET surface area of the electrodes with the different TiO<sub>2</sub> Structures.

TiO <sub>2</sub> morphology	BET (m <sup>2</sup> /g)
P20	72.21
P20-450	28.11
NR	8.17

As can be seen from Table 2, nanorod structures (NR) have the lowest surface area which originates from the micron lengths of these structures in comparison with nanoparticulate

structures of P20 and P20-450 samples (see Figure 1). Regarding the smaller surface area of NR structures, less QDs deposition and consequently lower current densities is expected in these structures while they have the highest current densities (Table 1). For more clear investigation, IPCE measurement was used to measure the photovoltaic properties of the cells more precisely. Figure 5 shows the IPCE results from P20, P20-450 and NR structures. As it can be seen from Figure 5 there is a red shift in IPCE data for the cells with nanorods structures.

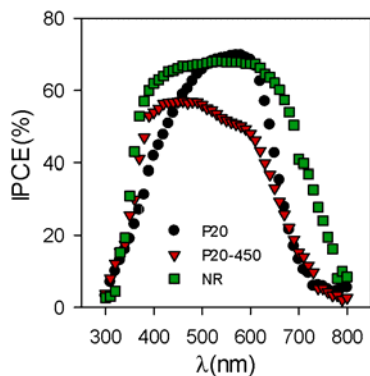


**Fig. 5.** IPCE curve for SILAR sensitized cells with various structures.

Diffuse reflectance spectrum of the samples with various structures is presented in Figure 6. According to this figure, the micron size of nanorods has enhanced the light scattering and consequently increases the light absorption especially in long wavelengths which leads to a red shift in IPCE (Figure 5).

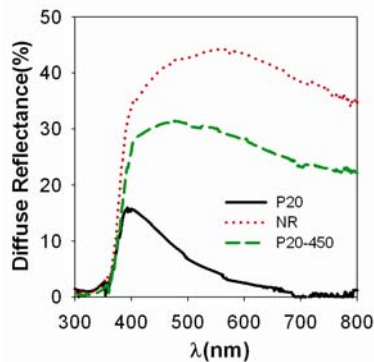


**Fig. 6.** Diffuse reflectance spectrum for various anode structures before sensitization by CdSe QDs.

To better understand the characteristic of the cells explained before, applied bias voltage decay was carried out on QDSCs under dark condition and their electron lifetime,  $\tau_n$ , was measured (Figure 7). According to Figure 7, the highest efficient cell with P20 structure (Table 1), has the lowest electron life time. According to Table 2, P20 structures have the highest surface area, which enhances the recombination rate of the electrons from photoanode with electrolyte. Consequently, higher recombination rate decreases the electron life time in P20 structures.

NR samples have the highest electron life time which arises from the micron length of nanorods decreasing the surface area in comparison with nanoparticulate structures (Table 2) and enhances the electron life time.

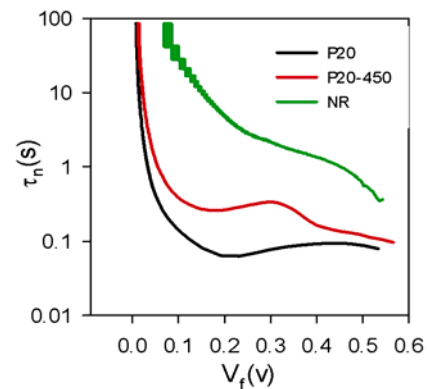


**Fig. 7.** Electron lifetime for SILAR sensitized cells; electron lifetime has obtained from ABVD measurements in dark conditions.

Comparing the efficiency of the cells with various structures (P20, P20-450 and NR) sensitized by SILAR method (see Table 1), indicate that all structures have rather high efficiencies while their structure is completely different. As discussed before, these cells have different scattering properties, surface area and electron life times while according to Table 1, all cells have the efficiencies higher than 2.65 %. Our results indicate that good efficiencies can be obtained by SILAR deposition method for various cells, although their photoanode is different in properties like: morphology, surface area, pore size and scattering. These results show that SILAR deposition can be introduced

as an effective simple method toward making high efficiency solar cells.

#### 4. Conclusions

We have made CdSe QDSCs with various photoanode structures. High power conversion efficiencies from 2.65 to 2.89 % were obtained for the cells sensitized by SILAR method. We have shown that SILAR sensitizing at room temperature can be introduced as an effective method to make efficient cells with various photoanode structures. Unique properties of SILAR method and rather high efficiencies obtained here point out that SILAR deposition is a promising method to make high efficient quantum dot sensitized solar cells in near future.

#### 5. References

- O'regan B., Gratzel M. A low-cost, high-efficiency solar cell based on dye-sensitized. *Nature*, 1991, 353, 737-740.
- Alivisatos A.P. Semiconductor clusters, nanocrystals, and quantum dots. *Science* 271, 1996, 5251, 933-937.
- Yu W.W., Qu L., Guo W., Peng X. Experimental determination of the extinction coefficient of CdTe, CdSe, and CdS nanocrystals. *Chem of Materials* 15, 2003, 14, 2854-2860.
- Diguna L. J., Shen Q., Kobayashi J., Toyoda T. High efficiency of CdSe quantum-dot-sensitized TiO<sub>2</sub> inverse opal solar cells. *App Physics Letters* 91, 2007, 2, 023116-023116.
- Ellingson R.J., Beard M.C., Johnson J.C., Yu P., Micic O.I., Nozik A.J., Shabaev A., Efros A.L. Highly efficient multiple exciton generation in colloidal PbSe and PbS quantum dots. *Nano letters* 5, 2005, 5, 865-871.
- Barea E.M., Shalom M., Giménez S., Hod I., Mora-Seró I., Zaban A., Bisquert J. Design of injection and recombination in quantum dot sensitized solar cells. *J of the American Chem Society* 132, 2010, 19, 6834-6839.
- Bisquert J., Cahen D., Hodes G., Rühle S., Zaban A. Physical chemical principles of photovoltaic conversion with nanoparticulate, mesoporous dye-sensitized solar cells. *The J of Physical Chem B*, 2004, 108, 24, 8106-8118.
- Braga A., Giménez S., Concina I., Vomiero A., Mora-Seró I. Panchromatic sensitized solar cells based on metal sulfide quantum dots grown directly on nanostructured TiO<sub>2</sub> electrodes. *The J of Physical Chem Letters*, 2011, 2, 5, 454-460.
- Diguna L.J., Murakami M., Sato A., Kumagai Y., Ishihara T., Kobayashi N., Shen Q., Toyoda T. Photoacoustic and photoelectrochemical characterization of inverse opal TiO<sub>2</sub> sensitized with CdSe quantum dots. *Japanese J of App physics*, 2006, 45, 6S, 5563.
- Giménez S., Mora-Seró I., Macor L., Guijarro N., Lana-Villarreal T., Gómez R., Diguna L.J., Shen Q., Toyoda T., Juan Bisquert. Improving the performance of colloidal quantum-dot-sensitized solar cells. *Nano Tech*, 2009, 20, 29, 295204.
- Hodes G. Comparison of dye-and semiconductor-sensitized porous nanocrystalline liquid junction solar cells. *The J of Physical Chem C*, 2008, 112, 46, 17778-17787.
- Mora-Seró I., Gimenez S., Fabregat-Santiago F., Gomez R., Shen Q., Toyoda T., Bisquert J. Recombination in quantum dot sensitized solar cells. *Accounts of Chem Research*, 2009, 42, 11, 1848-1857.
- Zhang Q., Guo X., Huang X., Huang S., Li D., Luo Y., Shen Q., Toyoda T., Meng Q. Highly efficient CdS/CdSe-sensitized solar cells controlled by the structural properties of compact porous TiO<sub>2</sub> photoelectrodes. *Physical Chem Chemical Physics* 13, 2011, 10, 4659-4667.
- Kamat P.V. Quantum dot solar cells. Semiconductor nano crystals as light harvesters. *The J of Physical Chem C*, 2008, 112, 48, 18737-18753.
- Kamat P.V., Tvrdy K., Baker D.R., Radich J.G. Beyond photovoltaics: semiconductor nanoarchitectures for liquid-junction solar cells. *Chem Reviews*, 2010, 110, 11, 6664-6688.
- Kongkanand A., Tvrdy K., Takechi K., Kuno M., Kamat P.V. Quantum dot solar cells. Tuning photoresponse through size and shape control of CdSe-TiO<sub>2</sub>

- architecture. *J of the American Chem Society*, 2008, 130, 12, 4007-4015.
17. Lee H.J., Wang M., Chen P., Gamelin D.R., Zakeeruddin S.M., Grätzel M., Nazeeruddin M.K. Efficient CdSe quantum dot-sensitized solar cells prepared by an improved successive ionic layer adsorption and reaction process. *Nano letters*, 2009, 9, 12, 4221-4227.
  18. Lee H.J., Bang J., Park J., Kim S., Park S.M. Multilayered semiconductor (CdS/CdSe/ZnS)-sensitized TiO<sub>2</sub> mesoporous solar cells: all prepared by successive ionic layer adsorption and reaction processes. *Chem of Mat*, 2010, 22, 19, 5636-5643.
  18. Lee Y.L., Lo Y.S. Highly Efficient Quantum-Dot-Sensitized Solar Cell Based on Co-Sensitization of CdS/CdSe. *Advanced Functional Materials*, 2009, 19, 4, 604-609.
  19. González-Pedro V., Xu X., Mora-Sero I., Bisquert J. Modeling high-efficiency quantum dot sensitized solar cells. *ACS Nano*, 2010, 4, 10, 5783-5790.